

Direct Measurement of the Penetration of Free Chains into a Tethered Chain Layer

Lay-Theng Lee¹ and Michael S. Kent²

¹Laboratoire Léon Brillouin, C.E. Saclay, 91191 Gif-sur-Yvette Cedex, France

²Sandia National Laboratories, P.O. Box 5800, Albuquerque, New Mexico 87185

(Received 22 May 1997)

Direct measurements of the penetration of free chains into a layer of tethered chains in good solvent conditions are reported. The segmental profiles of both the tethered chains ($N = 1625$ monomer units) and the free chains ($P = 413$ and 3846 monomer units) are obtained by neutron reflection. At 6 vol. %, the free chains penetrate the tethered layer at low surface density (σ), but are progressively excluded from the layer with increasing σ . At the highest σ ($\sigma\pi R_g^2 \cong 12$) there remains significant penetration into the layer for both values of P ; however, the form of the profile is strikingly different. [S0031-9007(97)04197-5]

PACS numbers: 61.41.+c, 61.12.-q

Layers of tethered chains, polymer chains which are attached by one end to a surface or interface, have important technological applications [1–3]. Polymer brushes thus formed are employed in such diverse areas as adhesion, lubrication, colloidal stabilization, chromatography, and drug delivery. A number of important systems involve layers of tethered chains which are in contact with a solution of free chains, such as colloidal suspensions, micelle-forming solutions of block copolymers and homopolymers, and biological systems. In such systems, the degree of penetration of free chains into the tethered layers can strongly affect critical properties such as the interaction potential between colloidal particles, the phase behavior of block copolymers in multicomponent solutions, or the adsorption of proteins onto surfaces. For example, a depletion of free chains between two polymer brush-coated colloidal particles has been shown to lead to a weak attractive force which strongly affects the degree of dispersion [4].

Several theoretical approaches have been employed to describe such systems. Initially, de Gennes [5] used a scaling approach to outline the major regimes and power law dependencies, and pointed out the fundamental significance of the degree of penetration of free chains into a brush. More detailed self-consistent field (SCF) calculations [4,6] provided further quantitative details, yielding weaker dependencies in addition to the power law behavior. Both treatments lead to three major regimes for $P < N$, where P and N are the degrees of polymerization of the free and tethered chains, respectively. These regimes are outlined here for the case of fixed free chain concentration (Φ) and varying surface density of tethered chains (σ), as is the case in the experiments described below. In regime I, σ is very high such that the average segmental concentration in the brush is much greater than Φ , and the structure of the brush is not affected by the free chains. At lower σ , where the average segmental concentration in the brush is comparable to or less than Φ , the presence of the free chains leads to a contraction of the brush relative to the height in pure solvent. However, the contraction can arise in two different ways.

In regime II the free chains do not penetrate the brush, and the contraction is due to osmotic equilibration between the solution and the brush. At values of σ still lower but yet sufficiently large to form a strongly stretched brush, the free chains penetrate the brush and screen the excluded volume interactions (regime III). With increasing P , regime II increases at the expense of regime III. For $P \gg N$ it is predicted that the free chains do not penetrate the tethered layer and regime III disappears.

It must be noted that the quantitative predictions of the above theories are relevant only for the asymptotic limit of high σ , where the chains are strongly stretched [1–3]. In this limit, Gast and Leibler [4] concluded that regime III is not relevant for most practical systems, since significant penetration of free chains into a strongly stretched brush is predicted only for $P \ll N$. However, it is now known that the asymptotic regime corresponds to very high reduced surface densities Σ ($= \sigma\pi R_g^2$ where R_g is the dilute solution free chain radius of gyration) and that in practice most systems do not fall into this limiting regime [7–9]. We show below that for $\Sigma < 12$ the free chains indeed penetrate the brush to a much greater extent than is predicted in the asymptotic limit.

The model tethered chain layer in this work is a Langmuir monolayer of highly asymmetric polydimethylsiloxane-polystyrene (PDMS-PS) diblock copolymers. The copolymer monolayer is spread onto the surface of a solution of free PS chains mixed with ethyl benzoate (EB), a good solvent for PS. The short PDMS blocks lie on the surface of EB, anchoring the copolymer to the surface due to the low surface energy of PDMS relative to EB. The large PS blocks dangle into the sub-phase and constitute the tethered layer [10].

It has been shown previously that the present systems begin with a contracted brush at the lowest σ , and reach brush heights approaching those obtained in pure EB at the highest σ [11]. Since either of two mechanisms (regimes II and III) can lead to contraction of the tethered layer, the degree of penetration of free chains into the brush cannot be determined from variations in the height

of the tethered layer alone. Below we report the first measurements of both the tethered and free chain segmental profiles, providing a direct measurement of the degree of penetration.

The measurement of the segmental profiles of both the tethered and free chains is achieved with neutron reflectivity using selective deuteration. Since protonated PS is contrast matched with EB, the profile of the deuterated component can be obtained unambiguously. In the first contrast scheme, the free PS chains are deuterated and the PS blocks are protonated. The deuteration is reversed in the second scheme. The molecular weights are nearly the same in the two contrast schemes, enabling a direct comparison. The profiles are obtained as a function of Σ at fixed Φ . The comparison of tethered and free chain profiles is made for both $P < N$ and $P > N$. The PDMS block has no effect on the reflectivity as its neutron scattering length density is nearly matched with that of air.

The protonated PDMS-PS copolymer 8-166 (where the numbers denote the molecular weight of each block in kg/mol) and the deuterated (d8) PS homopolymers (40 and 400 kg/mol, or 40K and 400K) were purchased from Polymer Source (Quebec, Canada). The PDMS-PS (d8) copolymer 21-169 and the protonated PS homopolymers (43 and 400 kg/mol) were obtained from Polymer Standard Service (Mainz, Germany). All polymers have a polydispersity index of 1.1 or less. Ethyl benzoate was obtained from Aldrich and redistilled before use. The PDMS-PS monolayers were spread from a dry grain of the copolymer deposited onto the surface of the PS/EB subphase. The copolymer surface density was then increased or decreased by further addition of grains or aspiration of the surface, respectively. The surface layer obtained in this manner is stable, and the pressure isotherm is reversible [7]. The surface pressure was measured using the Wilhelmy plate method in order to monitor the spreading process and control the surface density. The concentration of free chains was fixed at approximately 6 vol. %.

Neutron reflectivity experiments were performed on the DESIR reflectometer (LLB, Saclay) which operates in the time-of-flight mode. The incident angle was $\sim 0.6^\circ$, with an angular resolution of about 5%. For analysis of the data, reflectivity was calculated from model profiles using the optical matrix method, with a Debye-Waller factor, typically 3 Å, employed at the air surface to account for roughness due to capillary waves. Best fits were obtained using a nonlinear least squares fitting algorithm (Marquardt).

Representative reflectivity curves from the first contrast scheme for the case of $P < N$ (40K deuterated free chains) are shown in Fig. 1(a). The data are presented as the ratio of the reflectivity from the monolayer-covered surface to the calculated Fresnel reflectivity for a bare subphase of uniform composition equal to Φ . Curves are shown for Σ ranging up to 12. While the tethered chains are strongly interacting at $\Sigma \cong 12$, such systems are still far from the asymptotic regime [7,8].

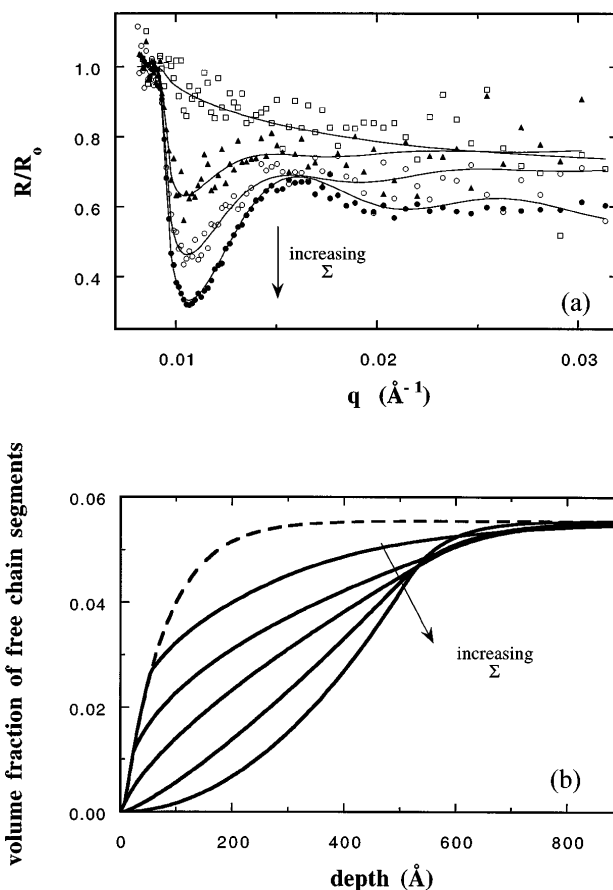


FIG. 1. (a) Representative reflectivity data for 40K deuterated free PS chains (~ 6 vol. %) and 170K protonated tethered PS blocks. R_0 is the calculated Fresnel reflectivity for a bare subphase of uniform composition equal to Φ . The copolymer surface density ranges up to $\Sigma \cong 12$. Open squares indicate reflectivity for $\Sigma = 0$. (b) Segmental concentration profiles for the 40K free PS chains. The dashed curve indicates the free chain profile for $\Sigma = 0$. With increasing Σ , the free chains are progressively excluded from the surface region.

The segmental profiles of the free *d*-PS chains are shown in Fig. 1(b). With no copolymer present, the free PS chain segments are depleted from the surface over a distance of ~ 60 Å [12]. This effect is due to the entropic penalty for chains which reside near a repulsive wall, and has been examined in detail previously [13,14]. With increasing Σ , the depth of the depleted zone increases and the shape of the free chain profile changes dramatically. At low Σ , the free PS chain profile is primarily affected at depths greater than 100 Å. This indicates that free chain segments are first expelled from the body of the tethered layer rather than the near surface region. At higher Σ , the gradient in the free chain profile at the surface becomes strongly affected, decreasing rapidly toward zero at the highest Σ values examined. In addition, with increasing Σ the shape of the profile changes from concave to convex, tending toward the exponential form predicted in the asymptotic limit [6]. The depth of the depletion zone becomes nearly independent of Σ at the highest values examined, saturating at roughly 600 Å. Thus, these results

clearly show significant free chain penetration at low Σ (region III), and progressive exclusion of mobile chains from the body of the brush with increasing Σ .

Representative reflectivity curves for the case of $P > N$ (400K deuterated free chains) are shown in Fig. 2(a). Curves are shown covering the same range of Σ as in Fig. 1(a). Interestingly, the form of the reflectivity curve for the 400K free PS chains at $\Sigma > 0$ is very different than that observed for the 40K free PS chains. Rather than a single peak, several are observed, and the peaks are sharper than those in Fig. 1(a).

The profiles for the 400K free chains obtained from these data are shown in Fig. 2(b). At $\Sigma = 0$, the free PS segments are depleted from the surface over nearly the same distance as observed for the 40K free chains in Fig. 1. This is expected since the characteristic length of the semidilute free chain solution is determined by Φ , and is independent of P . As in Fig. 1(b), Fig. 2(b) also shows progressive exclusion of free chains from the body of the

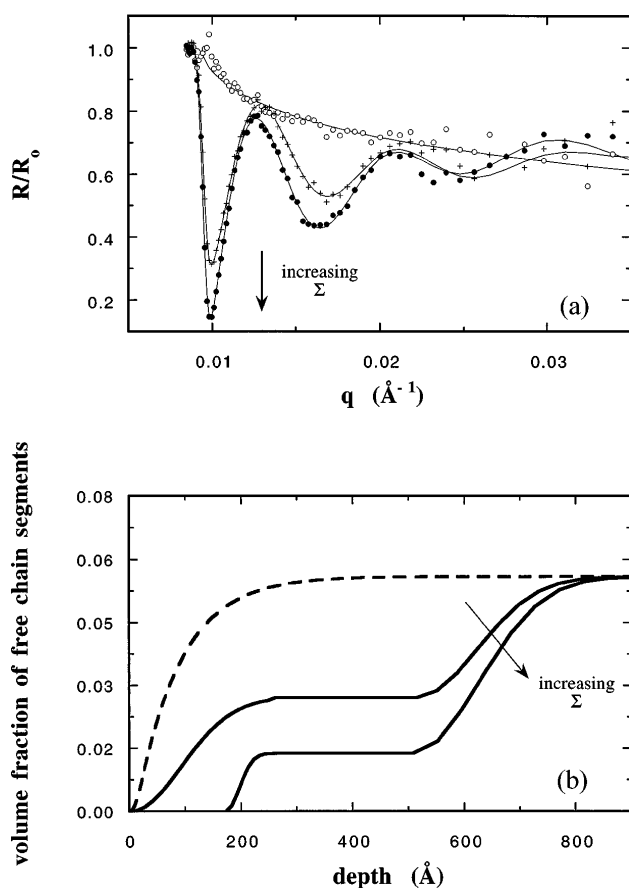


FIG. 2. (a) Representative reflectivity data for 400K deuterated free PS chains (~ 6 vol.%) and 170K protonated tethered PS blocks. The range of copolymer surface density is the same as that in Fig. 1. Open squares indicate reflectivity for $\Sigma = 0$. (b) Segmental concentration profiles for the 400K free PS chains. The dashed curve indicates the free chain profile for $\Sigma = 0$. As for the 40K PS chains, the free chains are progressively excluded from the surface region with increasing Σ . However, the form of the free chain profile at $\Sigma > 0$ is much different than for the 40K free chains.

brush with increasing Σ . However, in addition to this trend several surprising features are observed. It is remarkable that at the highest Σ , there remains significant penetration into the body of the brush for long free chains ($P/N = 2.4$) as was the case for short free chains ($P/N = 0.25$). Moreover, in contrast to the profiles in Fig. 1(b), those for the 400K free chains contain a plateau region within the body of the tethered layer. Furthermore, at the highest Σ , the segmental concentration drops abruptly to zero at ~ 200 Å from the surface, indicating complete exclusion of free chain segments within that region.

Corresponding tethered chain profiles for the systems in Figs. 1 and 2 have been obtained using the second contrast scheme. In Fig. 3 we show only the data obtained at $\Sigma \cong 12$ in the 400K PS solution along with reflectivity from the tethered d -PS layer in pure EB. Corresponding profiles are shown in the inset. In contrast to Figs. 1(a) and 2(a), in this contrast scheme the reflectivity curves for the tethered layer in the 400K and 43K solutions (data for 43K solution not shown) are nearly identical, except for rather subtle variations in the sharpness of the oscillations. This indicates that the body of the tethered chain profile is nearly the same for both free chain lengths. The sharpness of the oscillations is related to the magnitude of the tail of the profile. The exponential tail is most pronounced in pure EB, smaller in the 43K PS solution, and even further reduced in the 400K PS solution. The layer heights for the full range of Σ have been reported previously [11]. Defined by extrapolation of the body of the profile to zero volume fraction, the layer heights were found to be nearly the same in the 6% 43K and 400K solutions at all Σ values. The layers are contracted roughly 30% relative to that in pure EB at low Σ but approach that in pure EB at $\Sigma \cong 12$.

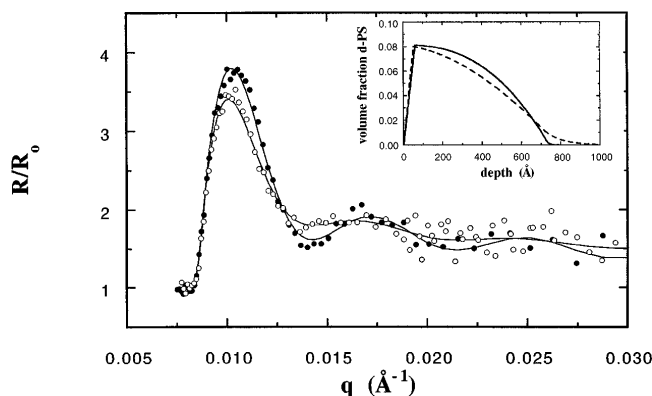


FIG. 3. Reflectivity data for tethered d -PS chains at $\Sigma = 11.0$ in pure EB (open circles) and at $\Sigma = 11.6$ in a 6 vol.% solution of 400K protonated PS (filled circles). R_0 is the calculated Fresnel reflectivity for the subphase in the absence of the copolymer. In contrast to the data in Figs. 1(a) and 2(a), little variation is seen in the reflectivity for different free chain lengths in this contrast scheme (reflectivity for the tethered d -PS chains in the 43K PS solution not shown). The inset shows the segmental concentration profiles for the tethered d -PS chains in pure EB (dashed line) and in the 6 vol.% solution of 400K protonated PS (solid line).

Direct comparisons of the profiles for the tethered blocks and the free PS chains for $\Sigma \cong 12$ are displayed in Figs. 4(a) (40K free chains) and 4(b) (400K free chains). In both cases there remains significant penetration of free chains into the body of the brush, although the degree of penetration is greater for the smaller free chains. Profiles calculated from the analytic SCF theory of Zhulina *et al.* [6] in the asymptotic limit are also displayed in Figs. 4(a) and 4(b) for comparison. Much greater free chain penetration into the brush is observed in the experimental profiles than is predicted in the asymptotic theory. On the other hand, numerical SCF calculations modeling the conditions of the 40K free chain solution ($\Sigma \cong 12$) have shown significant penetration into the layer, similar to that in Fig. 4(a) [15]. Significant free chain penetration has also been observed in recent molecular dynamics simulations [16] for very similar conditions. The significant penetration of free chains into the layer at $\Sigma \leq 12$ is further evidence that such systems are far from the asymptotic regime, and that

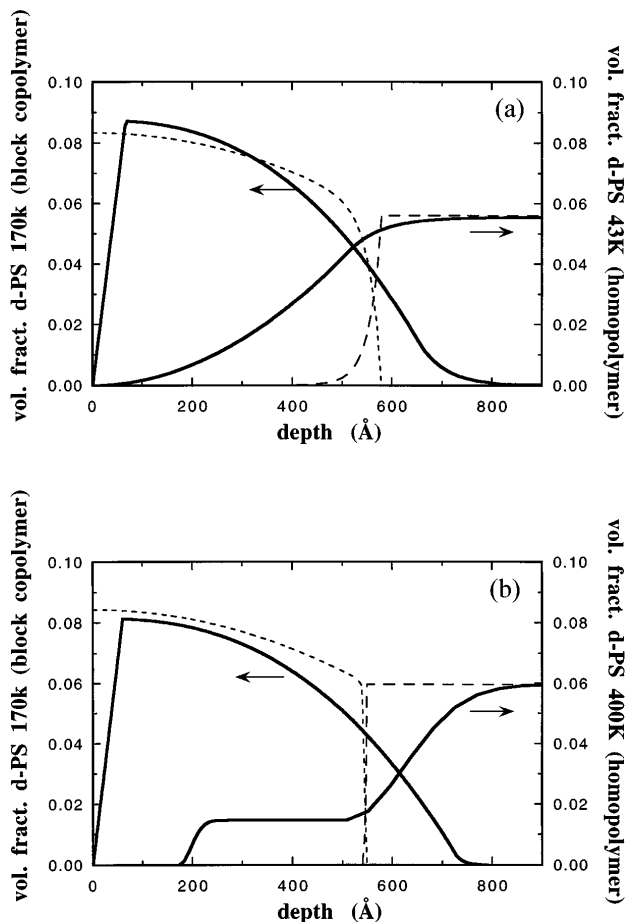


FIG. 4. Comparison of the segmental profiles for the 170K tethered PS block and (a) 40K and (b) 400K free PS chains at $\Sigma = 12$. While the free chains are largely excluded from the surface region, for both molecular weights there is more penetration of free chains into the brush than is predicted by SCF calculations in the asymptotic limit of strong stretching (dashed lines). The degree of penetration at $\Sigma \cong 12$ is lower for the 400K chains than for the 40K chains.

numerical SCF calculations are required for an accurate description [8,15,17]. Another consequence of the above is that regime II does not exist for the Σ range of most practical systems, but rather regime III (penetration of mobile chains) is most relevant. Finally, the fact that total exclusion of free chain segments from the near surface region is only achieved for certain Σ and P/N has important implications for systems involving free chains which interact with a surface, such as for protein adsorption onto biosurfaces.

This work was partially supported by the U.S. Department of Energy under Contract No. DE-AC04-94AL85000.

- [1] A. Halperin, M. Tirrell, and T.P. Lodge, *Adv. Polym. Sci.* **100**, 31 (1992).
- [2] G.S. Grest and M. Murat, in *Monte Carlo and Molecular Dynamics Simulations in Polymer Science*, edited by K. Binder (Oxford University Press, New York, 1995).
- [3] I. Szleifier, *Adv. Chem. Phys.* **94**, 165 (1996).
- [4] A.P. Gast and L. Leibler, *Macromolecules* **19**, 686 (1986).
- [5] P.G. de Gennes, *Macromolecules* **13**, 1069 (1980).
- [6] E.B. Zhulina, O.V. Borisov, and V.A. Pryamitsin, *J. Colloid. Interface Sci.* **137**, 495 (1990); E.B. Zhulina, O.V. Borisov, and L. Brombacher, *Macromolecules* **24**, 4679 (1991).
- [7] M.S. Kent, L.T. Lee, B.J. Factor, F. Rondelez, and G. Smith, *J. Chem. Phys.* **103**, 2320 (1995).
- [8] R. Baranowski and M.D. Whitmore, *J. Chem. Phys.* **103**, 2340 (1995); M.D. Whitmore and J. Noolandi, *Macromolecules* **23**, 3321 (1990).
- [9] To our knowledge, all the data for chains tethered onto surfaces from dilute solution fall into the range of $\Sigma < 12$. It has been shown via the dependencies of the layer height on σ and N that this range of Σ does not fall within the asymptotic regime [7,8]. Much higher Σ can be obtained by tethering from a concentrated solution or melt [18,19]. However, in many practical cases this is not feasible for economic reasons.
- [10] Since the surface energy of EB is lower than that of PS, the PS segments do not adsorb at the air surface.
- [11] L.T. Lee, B.J. Factor, M.S. Kent, and F. Rondelez, *J. Chem. Soc. Faraday Discuss.* **98**, 139 (1994).
- [12] The shape of the profile is consistent with the squared hyperbolic tangent form predicted by mean-field theory [13], although the present data for $\Sigma = 0$ are not very discriminating in that regard.
- [13] A. Silverberg, *Pure Appl. Chem.* **26**, 583 (1971).
- [14] L.T. Lee, O. Guiselin, A. Lapp, B. Farnoux, and J. Penfold, *Phys. Rev. Lett.* **67**, 2838 (1991).
- [15] C.M. Wijmans and B.J. Factor, *Macromolecules* **29**, 4406 (1996).
- [16] G. Grest (private communication).
- [17] C.M. Wijmans, E.B. Zhulina, and G.J. Fleer, *Macromolecules* **27**, 3238 (1994).
- [18] P. Auroy, L. Auvray, and L. Léger, *Macromolecules* **24**, 5158 (1991).
- [19] A. Karim, S.K. Satija, J.F. Douglas, J.F. Ankner, and L.J. Fetters, *Phys. Rev. Lett.* **73**, 3407 (1994).